DOI 10.2478/ama-2025-0051

acta mechanica et automatica, vol.19 no.3 (2025)
Special Issue "New Trends in Biomedical Engineering"

MECHANO-RESPONSIVE POLYAMPHOLYTE HYDROGELS WITH STRAIN-STIFFENING PROPERTY FOR WOUND CLOSURE APPLICATIONS

Gustini GUSTINI*/, Kaprawi SAHIM**, Ida SRIYANTI***, Irmawan IRMAWAN******

*Faculty of Engineering, Doctoral Program of Mechanical Engineering, University of Sriwijaya,
Indralaya, South Sumatera, 30662, Indonesia
**Faculty of Engineering, Department of Mechanical Engineering, University of Sriwijaya,
Indralaya, South Sumatera, 30662, Indonesia
***Faculty of Education, Department of Physics Education, University of Sriwijaya,
Indralaya, South Sumatera, 30662, Indonesia
****Faculty of Engineering, Department of Electrical Engineering, University of Sriwijaya,
Indralaya, South Sumatera, 30662, Indonesia

gustini@unsri.ac.id, kaprawi@unsri.ac.id, ida_sriyanti@unsri.ac.id, irmawan@unsri.ac.id

received 02 October 2024, revised 04 June 2025, accepted 16 June 2025

Abstract: Strain-stiffening properties are the most applied in mechano-responsive hydrogels that respond to external mechanical forces. Wounds subjected to frequent deformations are difficult to treat because external mechanical forces can easily interfere with the healing process. The strain-stiffening property reduces the effect of external mechanical forces and acts as a damper response to these forces. Therefore, tough wound closure with stimuli-responsive strain-stiffening release properties for treating these wounds is highly desirable. In this study, we developed a strain-stiffening polyampholyte hydrogel that aims to accelerate wound closure as a damper of external mechanical forces. Self-assembly technique was used to fabricate a polyampholyte hydrogel. The differential modulus of the polyampholyte hydrogel exhibited strain-stiffening property. In addition, the mechanical stress applied to the polyampholyte hydrogel increased strain-stiffening penetration into the skin tissue. The strain-stiffening properties of the polyampholyte hydrogel also demonstrated an excellent damping of external mechanical forces to accelerate wound closure. The developed strain-stiffening hydrogel is promising for wound closure applications in wounds subjected to frequent deformations from external mechanical forces.

Key words: strain-stiffening property; self-assembly; differential modulus; polyampholyte hydrogel; wound closure

1. INTRODUCTION

Mechanical responsiveness plays an essential role in many biomechanical processes and is common in biological systems [1, 2]. Over the last two decades, significant effort has been made for developing biomimetic mechano-responsive hydrogels capable of altering their physical and chemical characteristics in response to external mechanical stimuli. In this study, a bioinspired hydrogel was developed to replicate tissue-like mechano-responsiveness, exhibiting strain-stiffening and stress-induced differential modulus adaptation. Biomimetic self-assembly endows the material with structural stability, biocompatibility, and enhanced mechanical performance in wound closure applications. Owing to the apparent combination of tissue resemblance and mechano-responsive capabilities, this type of hydrogel offers significant advantages in a wide range of biomedical applications. Based on preclinical research and clinical reports implicating mechanical tension effects, scar formation would be inhibited if mechanical forces were actively offset through stress shielding by activating mechano-responsiveness across the wound [3]. Mechano-responsive materials are also implicated in practically all physiological processes, such as homeostasis and development of organs and tissues [4-7]. It is widely recognized that mechano-responsive materials modulate skin and wound behavior [4, 8-10]. Mechano-responsive materials modulate skin and wound closure through mechanotransduction and extracellular matrix (ECM) remodeling pathways, particularly involving β-integrins. These mechanisms regulate cellular responses to mechanical stimuli, enhancing tissue repair and creating a supportive environment for wound closure. Mechano-responsive hydrogels are categorized into several groups based on properties that change in response to mechanical stimuli, such as viscosity, color, and strength. The most studied response properties in hydrogel systems include strain-stiffening, mechanochromism, self-healing, and shear thinning [1, 11-17]. Strain-stiffening is a mechanical response with a nonlinear force-extension relation. A material can exhibit strain-stiffening when stretched, and a positive strain causes an increase in stiffness along the strain direction [18, 19]. Strain-stiffening hydrogel mimics the physiological features of biological tissues, making them intriguing options for tissue scaffolds, artificial tissues, and wound closure [20-22]. However, if the external stimuli reach sufficiently high levels, it can lead to mechanical failure (fracture) and damage the skin [20]. Strain-stiffening synthetic materials consist of two or more separate networks with varying stiffnesses for synergizing firmness and softness [11, 23].

To the best of our knowledge, only a few studies have shown unique strain-stiffening properties for enhanced wound closure in synthetic materials as most synthetic materials exhibit negligible strain-stiffening properties. Previous research has resulted the development of wound dressings using polyisocyanopeptides that show strain-stiffening properties [21, 22]. The enhancement or acceleration of wound dressing techniques has been the topic of many recent studies. However, studies regarding the use of strain-stiffening properties of mechano-responsive materials for wound-closure applications are very few. Polyampholyte polymers, such as poly (SA-co-TMA), have been widely used as antifouling materials to facilitate wound dressing by enhancing skin re-epithelialization of wounds after injury [24]. Mixed-charge copolymers composed of 3-sulfopropyl methacrylate (SA) and [2-(methacryloyloxy)ethyl] trimethylammonium (TMA) exhibit precise charge balance, high hydration capacity, protein antifouling, and antibacterial activity through their polyampholyte nature. Mechanically, the incorporation with polytetrafluoroethylene (ePTFE) membranes provides high tensile strength, elasticity, fatigue resistance, and dimensional stability, making them suitable for dynamic and load-bearing wound environments.

Herein, we report the design and preparation of a self-assembly (SAM) technique to enhance the mechanical and mechano-responsive properties of TSC polyampholytes. The TSC polyampholyte constitutes a cationic monomer of a 2-(Acryloyloxy ethyl) trimethylammonium chloride (TMA) and two anionic monomers, 3-sulfopropyl methacrylate potassium salt (SA) and 2-carboxyethyl acrylate (CAA), where T, S, and C represents the TMA, SA, and CAA monomers, respectively, and the number represents the molar ratio that includes a cross-linking triethylene glycol dimethacrylate network. The influence of SAM technique on the phase structure, mechanical and mechano-responsive properties was examined. The characteristics of the TSC polyampholytes were studied in detail using IR. An SAM of the TSC polyampholyte hydrogel displayed strain-stiffening properties. In addition, the effects of the TSC polyampholyte hydrogel on mediating the cell fate was studied and optimized. The results indicated that the strain-stiffening property would aim in solving the problem of wound-closure in static or dynamic mechanical environments.

2. MATERIALS AND METHODS

2.1. Preparation of the TSC polyampholyte based on the SAM approach

A typical SAM approach was used for the synthesis of TSC. We synthesized a new type of polyampholyte hydrogel $T_1S_xC_{1-x}$ by one-step copolymerization of a cationic monomer of TMA and two anionic monomers, SA and CAA. In Milk Q water, 80 μL of a 15% sodium metabisulfite solution and 80 μL of a 40% ammonium persulfate solution were used to begin polymerization, which was slightly different from that used in a previous study [25]. The polymerization procedure was then performed for 1 h at 60°C, after which the gel was cooled for 1 h at room temperature. Following SAM, an 8 M sodium hydroxide (NaOH) aqueous solution was filtered to assemble the TSC building blocks to obtain TSC polyampholyte (SAM).

2.2. Sample Characterizations

Infrared spectroscopy (IR) was performed using a Vertex 70 series spectrophotometer (Bruker Optics, USA). This spectrometer was used to study the secondary structure of TSC polyampholyte with different ratios were referred to as $T_1S_0C_1$, $T_1C_{0.5}S_{0.5}$, and $T_1S_1C_0$ samples.

2.3. Mechanical Characterizations

A tensile machine (FGS-50E-H, Japan) was used to investigate the tensile properties of the TSC polyampholyte. Uniaxial tensile tests were performed in accordance with the ISO 37 Type 3 standard. The strain-stiffening of the material was used to determine the mechanical performance [25]. The differential modulus (k') of hydrogel was assessed according to the following equation (1) [26].

$$k' = \frac{\partial\sigma}{\partial\gamma} \tag{1}$$

Here, k' denotes the differential modulus, defined as a function of stress (σ) and strain (γ), for the same hydrogel.

2.4. In vitro Cell culture

The viability of human dermal fibroblasts-adult HDF-a was quantitatively verified by using cell counting kit (CCK-8, Dojindo, Japan) assay on days 3 and 7. The HDF-a cells were seeded in 21 well-cultured plates and then immersed in a CCK-8 reagent-mixed solution at 37°C for 2 h. Finally, viability of HDF-a cell was determined using a plate reader and absorbance was measured at 450 nm. The nuclei of HDF-a cells were stained with 4',6'-diamidino-2-phenyl-indol (DAPI, Sigma-Aldrich). For cell morphology and viability observation, the samples were stained using fluorescein diacetate (FDA, Sigma-Aldrich) staining assays and photographed after 7 days.

HDF-a cell migration was studied using an in vitro wound closure scratch assay. Firstly, seed the HDF-a cell suspension into each well with the silicone culture insert using 200 μm as a physical barrier. Afterwards, removal of the culture insert will engender a clean cell-free gap. Incubate the dishes for 24 hours at 37°C and 5% CO_2 to allow the cells to migrate into [27]. Finally, measurement of cell migration in the central gap area was measured using Image J software.

2.5. Statistical analysis

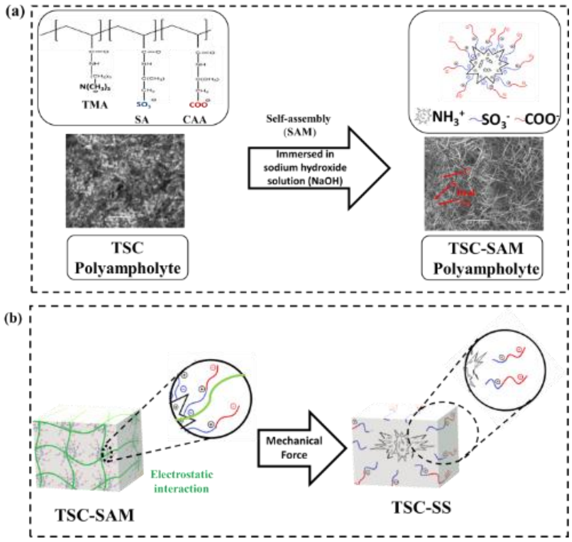

Scheme 1. Schematic Diagram Illustration (a) Preparation of TSC Polyampholyte hydrogel (b) Preparation of TSC-SS Polyampholyte under mechanical force (uniaxial stress)

All data were measured in five replicates (n = 5), unless specified otherwise, represented as the mean ± standard deviation. Statistical significance was indicated by (∗) for probability less than 0.05 ($P < 0.05$), (∗∗) for $P < 0.01$, (∗∗∗) for $P < 0.001$, and (∗∗∗∗) for $P < 0.0001$.

3. RESULT AND DISCUSSION

3.1. Preparation of the TSC polyampholyte based on the SAM approach

In this study, we used copolymerization to prepare TSC polyampholyte hydrogels. The positively charged T (TMA) is repulsive, whereas the negatively charged S (SA) and C (CAA) exert an attractive interaction. TSC polyampholytes were synthesized in three different types with varying numbers of S and C repeat units. In presence of S negatively charged, the $-SO_3^-$ strong anion (S) was exposed, thus increasing interaction with $-COO^-$ weak anion (C) on the TSC networks. After immersion in NaOH solution, negatively charged S and C interact with positively charged T to form structures in which S and C are located at the outer surface under physiological conditions. In presence of NaOH nanoparticles, the $-NH_3^+$ positively charged (T) was unexposed, thus preventing interaction with $-SO_3^-$ negatively charged (S) and $-COO^-$ negatively charged (C) on the TSC networks. This process, known as self-assembly (SAM) formation as shown in Fig. 1b, is depicted in Scheme 1a with an illustration. Thus, SEM imaging (Fig. 1) reveals that the self-assembly process promotes the formation of an interwoven fibrous network within the TSC polyampholyte hydrogel matrix, a feature that is lacking in the non-assembly control samples. These nanofibrillar structures result from the spontaneous organization of triblock copolymers into β-sheet-like domains, as further supported by FTIR analysis (Fig. 3).

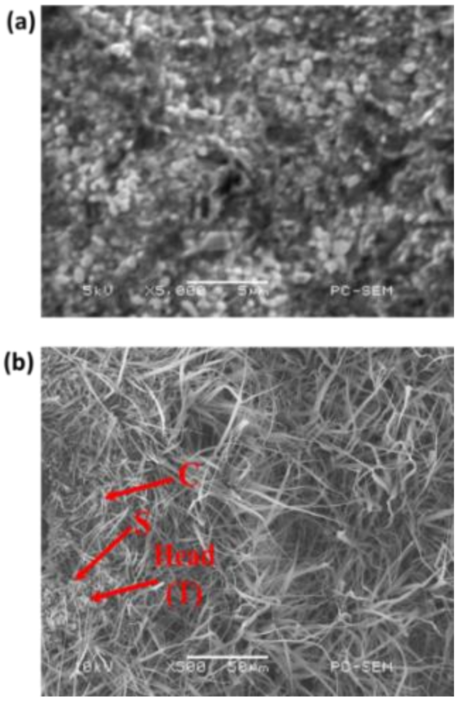

Fig. 1. Scanning electron microscopy (SEM) images of TSC polyampholyte hydrogel (a) before and (b) after self-assembly process

The C and S functional groups were protonated after immersion in aqueous 8 M NaOH. Mechanical force can weaken the electrostatic interaction between C and S, resulting in detachment from the complex in Scheme 1b.

The IR analysis results show that the absorption bands of the hydrogels are characteristic amide-I bands as shown in Fig. 2a-b below [28, 29].

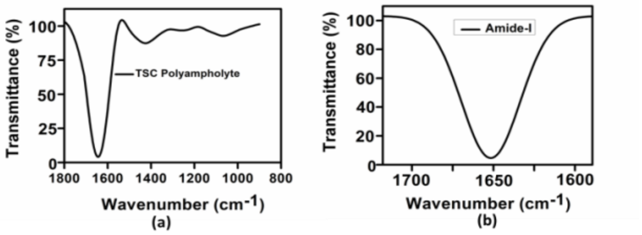

Fig. 2. Characterization of TSC polyampholyte (a) IR spectra of the TSC Polyampholyte the representative of the IR absorbance spectra of the TSC Polyampholyte (b) The amide-I band region (~1600-1700 cm^{-1})

The IR spectra in the amide-I band of TSC polyampholyte as shown in Fig. 3 with different ratios (Tab. 1). The amide-I induced pathogenic amyloid transitions that play an important role in immunological homeostasis during wound healing [30].

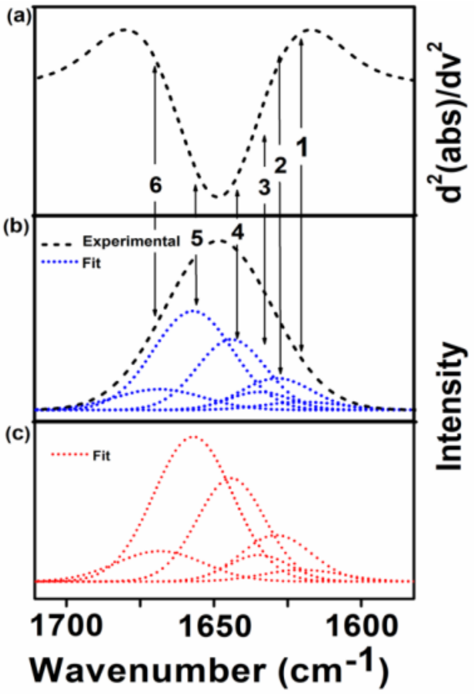

1	2	3	4	5	6
~1602 (Side chain)	~1611 (β-sheet)	~1623 (β-sheet)	~1635 (β-sheet)	~1656 (α-helix)	~1675 (β-turn)

Fig. 3. Spectra of protein secondary structure analysis (a) the IR absorbance spectra's second derivatives contained to the amide-I band (b) IR spectra in the amide-I were fitted by approximating the number and position, which experimental curve (···) and simulated fits (…) (c) Result simulated fits are the six Gaussian band prof.

Tab. 1. Amide-I number and position (cm^{-1}) of TSC polyampholyte

TSC polyampholyte	**Amide-I number and position (cm^{-1})**					
	1	2	3	4	5	6
$T_1S_1C_0$	~1601 (Side chain)	~1602 (Side chain)	~1617 (β-sheet)	~1633 (β-sheet)	~1651 (α-helix)	~1664 (β-turn)
$T_1S_{0.5}C_{0.5}$	~1602 (Side chain)	~1611 (β-sheet)	~1623 (β-sheet)	~1635 (β-sheet)	~1656 (α-helix)	~1675 (β-turn)
$T_1S_0C_1$	~1602 (Side chain)	~1619 (Side chain)	~1631 (β-sheet)	~1650 (α-helix)	~1665 (β-turn)	~1680 (β-turn)

3.2. Preparation of the TSC polyampholyte based on the SAM approach

A uniaxial tensile test was performed to validate the increase in the mechanical performance of the TSC polyampholytes. The TSC polyampholytes ($T_1S_xC_{1-x}$) with different molar concentrations are referred to as $T_1S_1C_0$, $T_1S_{0.5}C_{0.5}$, and $T_1S_0C_1$. In this study, a variety of TSC polyampholytes were manufactured with different SC molar concentrations, using both self-assembly (SAM) and non-self-assembly (N-SAM) techniques. The TSC (SAM) with the SAM technique exhibits strain-stiffening as opposed to TSC (N-SAM) with no self-assembly. $T_1S_{0.5}C_{0.5}$ (SAM) exhibits an optimal differential modulus as shown in Fig. 4. The experimental results thus suggest that strain-stiffening properties enhance the mechanical performance and mechano-responsiveness of TSC polyampholyte.

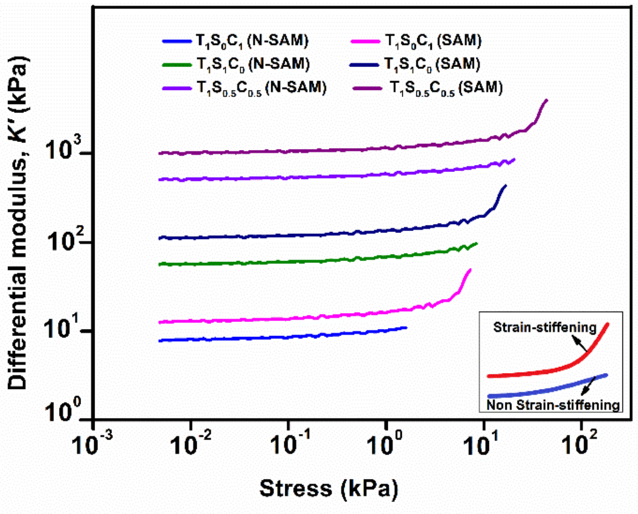

Fig. 4. Strain-stiffening curves of TSC polyampholyte

3.3. Strain-stiffening-mediated cell fate

Considering the results of the strain-stiffening analysis, it is possible to hypothesize that during tensile loading, cell bodies are pushed against the surroundings and contact each other, resulting in tensile resistance and strain-stiffening [25]. The current study reveals that the strain-stiffening property of tension may be considered to mediate cell fate. To evaluate the effect of strain-stiffening on the mediated cell fates, human dermal fibroblasts-adult (HDF-a) were cultured under controlled conditions, and no strain-stiffening (TSC-Non-SS) and strain-stiffening (TSC-SS) were calculated as Fig. 5. After 7 days of cultivation, HDF-a cells adhered well to the surface of the matrix. Strain-stiffening also guides the cell-cell-sensing process of cell adhesion [31]. Adhesion of cells (proliferation and differentiation) enhances with the strain-stiffening of TSC-SS as Fig. 5.

One interesting outcome was the effect of the TSC polyampholyte on the increase in HDF-a content. This effect can be explained by the strain-stiffening property of the TSC polyampholyte hydrogel. Strain-stiffening mediates cell spreading on the hydrogel matrix. Cell spreading of HDF-a cells enhances with the strain-stiffening of TSC polyampholyte (TSC-SS) as Fig. 6.

The results demonstrate that under tensile loading, cell bodies are compressed against their surrounding microenvironment, promoting cell-cell contact. This interaction enhances tensile resistance and increases cell stiffness. The resulting increase in stiffness induces strain-stiffening, a mechanical response that appears to critically influence cell fate determination.

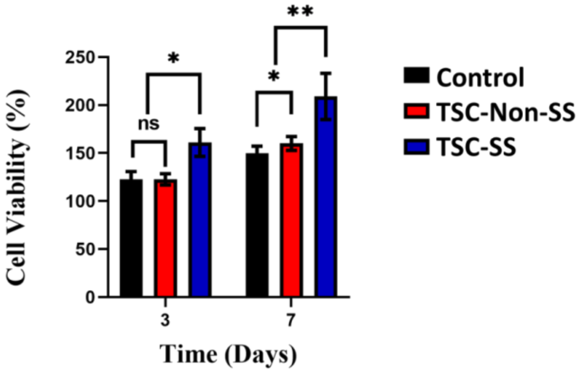

Fig. 5. The cell viability of HDF-a of the different culture plate (control), TSC-Non-SS polyampholyte and TSC-SS polyampholyte

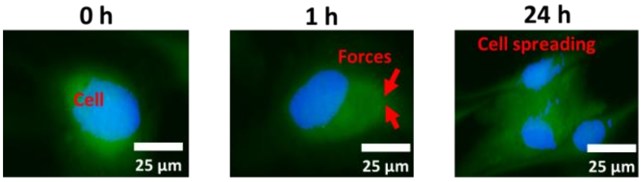

Fig. 6. The HDF-a cells spreading on strain-stiffening of TSC polyampholyte. Scale bar 25 µm

The strain-stiffening TSC could effectively mediate the cell migration than TSC-Non-SS and cultured plates after 24 hours treatment as Fig. 7.

TSC-SS demonstrated higher migrating activity, which could be represented as number of cells filling the central gap as Fig. 8. Furthermore, the strain-stiffening TSC could effectively mediate the cell fate of HDF-a to promote a general organizing principle during tissue development or regeneration. Overall, TSC-SS polyampholytes are promising for wound closure applications.

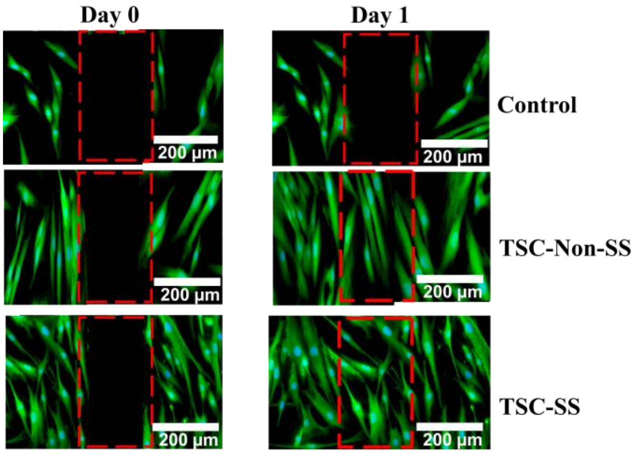

Fig.7. In vitro cell culture, strain-stiffening polyampholyte (TSC-SS), non-strain-stiffening polyampholyte (TSC-Non-SS) and control induce motility in HDF-a cells after 1 day. Scale bar = 200 µm

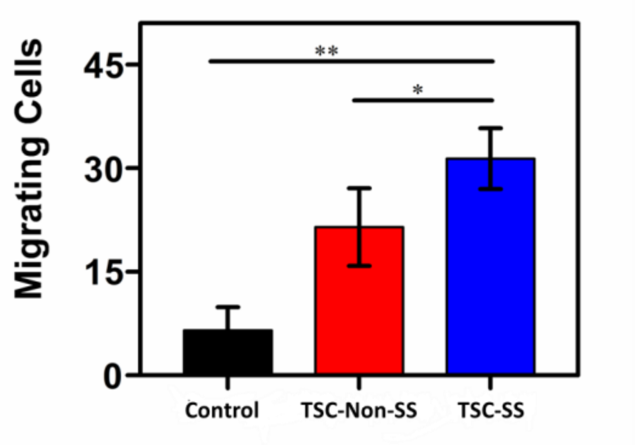

Fig. 8. Cell migration quantification of TSC polyampholyte

4. CONCLUSIONS

In this study, we developed mechano-responsive materials and a self-assembly (SAM) technique to evaluate the strain-stiffening property of TSC polyampholytes for wound closure applications. The TSC hydrogel has amide content, and its differential modulus, contributed to the excellent strain-stiffening property of the TSC polyampholyte. Therefore, strain-stiffening also guides mediated cell fate and is used to connect cells. In addition, the cell migration results indicated that the TSC-SS hydrogel took a shorter time to heal the wound than the TSC-non-SS hydrogel and significantly accelerated the wound closure process with less wound closure time. The strain-stiffening property is a damper response to external mechanical forces and promotes wound closure. Such tough strain-stiffening hydrogels hold great promise for treating wounds in static or dynamic mechanical environments.

REFERENCES

1. Chen J, Peng Q, Peng X, Han L, Wang X, Wang J, et al. Recent advances in mechano-responsive hydrogels for biomedical applications. ACS Appl Polym Mater. 2020;2(3):1092–107.
2. Lavrador P, Esteves MR, Gaspar VM, Mano JF. Stimuli-responsive nanocomposite hydrogels for biomedical applications. Adv Funct Mater. 2021;31(8):1–30.
3. Mascharak S, Griffin M, Chen K, Duoto B, Chinta M. Preventing Engrailed-1 activation in fibroblasts yields wound regeneration without scarring. Science (80-). 2021;372(6540):356.13-358.
4. Lin X, Bai Y, Zhou H, Yang L. Mechano-active biomaterials for tissue repair and regeneration. J Mater Sci Technol (Internet]. 2020;59(June):227-33.
Available from: https://doi.org/10.1016/j.jmst.2020.03.074
5. Panciera T, Azzolin L, Cordenonsi M, Piccolo S. Mechanobiology of YAP and TAZ in physiology and disease. Nat Rev Mol Cell Biol (Internet]. 2017;18(12): 758-70.
Available from: http://dx.doi.org/10.1038/nrm.2017.87
6. Armiger TJ, Lampi MC, Reinhart-King CA, Dahl KN. Determining mechanical features of modulated epithelial monolayers using subnuclear particle tracking. J Cell Sci. 2018;131(12):3–8.
7. Guilak F, Butler DL, Goldstein SA, Baaijens FP. Biomechanics and mechanobiology in functional tissue engineering. 2015;47(9):1933–40.
8. Wong VW, Akaishi S, Longaker MT, Gurtner GC. Pushing back: Wound mechanotransduction in repair and regeneration. J Invest Dermatol. 2011;131(11):2186–96.
9. Barnes LA, Marshall CD, Leavitt T, Hu MS, Moore AL, Gonzalez JG, et al. Mechanical forces in cutaneous wound healing: emerging therapies to minimize scar formation. Adv Wound Care. 2018;7(2): 47–56.
10. Aarabi S, Bhatt KA, Shi Y, Paterno J, Chang EI, Loh SA, et al. Mechanical load initiates hypertrophic scar formation through decreased cellular apoptosis. FASEB J. 2007;21(12):3250–61.
11. Zhang J, Keith AN, Sheiko SS, Wang X, Wang Z. To mimic mechanical properties of the skin by inducing oriented nanofiber microstructures in bottlebrush cellulose-graft-diblock copolymer elastomers. ACS Appl Mater Interfaces. 2021;13(2):3278–86.
12. Zhang W, Wu B, Sun S, Wu P. Skin-like mechanoresponsive self-healing ionic elastomer from supramolecular zwitterionic network. Nat Commun [Internet]. 2021;12(1).
Available from: http://dx.doi.org/10.1038/s41467-021-24382-4
13. Wang X-Y, Zhang J, Dong Y-B, Zhang Y, Yin J, Liu SH. Different structures modulated mechanochromism and aggregation-induced emission in a series of Gold (I) complexes [Internet]. Vol. 156, Dyes and Pigments. Elsevier Ltd; 2018. 74–81 hal. Available from: https://doi.org/10.1016/j.dyepig.2018.03.062
14. Norton AE, Abdolmaleki MK, Liang J, Sharma M, Golsby R, Zoller A, et al. Phase transformation induced mechanochromism in a platinum salt: a tale of two polymorphs. Chem Commun. 2020;56(70):10175–8.
15. Uman S, Dhand A, Burdick JA. Recent advances in shear-thinning and self-healing hydrogels for biomedical applications. J Appl Polym Sci. 2020;137(25):1–20.
16. Zandi N, Sani ES, Mostafavi E, Ibrahim DM, Saleh B, Shokrgozar MA, et al. Nanoengineered shear-thinning and bioprintable hydrogel as a versatile platform for biomedical applications. Biomaterials [Internet]. 2021;267:120476.
Available from: https://doi.org/10.1016/j.biomaterials.2020.120476
17. Seppala JE, Heo Y, Stutzman PE, Sieber JR, Snyder CR, Rice KD, et al. Characterization of clay composite ballistic witness materials. Time-, temperature-, and history-dependent properties. J Mater Sci. 2015;50(21):7048–57.
18. Ramos JRD, Travasso R, Carvalho J. Capillary network formation from dispersed endothelial cells: Influence of cell traction, cell adhesion, and extracellular matrix rigidity. Phys Rev E. 2018;97(1):1–11.
19. Van Oosten ASG, Vahabi M, Licup AJ, Sharma A, Galie PA, MacKintosh FC, et al. Uncoupling shear and uniaxial elastic moduli of semiflexible biopolymer networks: compression-softening and stretch-stiffening. Sci Rep. 2016;6(December 2015):1–9.
20. Op't Veld RC, Walboomers XF, Jansen JA, Wagener FADTG. Design considerations for hydrogel wound dressings: strategic and molecular advances. Tissue Eng - Part B Rev. 2020;26(3):230–48.
21. Op't Veld RC, Joosten L, van den Boomen OI, Boerman OC, Kouwer P, Middelkoop E, et al. Monitoring 111 In-labelled polyisocyanopeptide (PIC) hydrogel wound dressings in full-thickness wounds. Biomater Sci. 2019;7(7):3041–50.

22. op't Veld RC, van den Boomen OI, Lundvig DMS, Bronkhorst EM, Kouwer PHJ, Jansen JA, et al. Thermosensitive biomimetic polyisocyanopeptide hydrogels may facilitate wound repair. Biomaterials [Internet]. 2018;181:392–401. Available from: https://doi.org/10.1016/j.biomaterials.2018.07.038
23. Keith AN, Vatankhah-Varnosfaderani M, Clair C, Fahimipour F, Dashtimoghadam E, Lallam A, et al. Bottlebrush bridge between soft gels and firm tissues. ACS Cent Sci. 2020;6(3):413–9.
24. Jhong JF, Venault A, Liu L, Zheng J, Chen SH, Higuchi A, et al. Introducing mixed-charge copolymers as wound dressing biomaterials. ACS Appl Mater Interfaces. 2014;6(12):9858–70.
25. Gustini, Lin WC. Characterizations of the strain-stiffening property and cytotoxicity in the self-assembled polyampholyte hydrogel. J Mech Sci Technol. 2022;36(5):2653–61.
26. Wang Y, Xu Z, Lovrak M, le Sage VAA, Zhang K, Guo X, et al. Biomimetic strain-stiffening self-assembled hydrogels. Angew Chemie - Int Ed. 2020;59(12):4830–4.
27. Riahi R, Yang Y, Zhang DD, Wong PK. Advances in wound-healing assays for probing collective cell migration. J Lab Autom. 2012;17(1):59–65.
28. Ji Y, Yang X, Ji Z, Zhu L, Ma N, Chen D, et al. DFT-calculated IR spectrum amide I, II, and III band contributions of N-methylacetamide fine components. ACS omega. 2020;5(15):8572-8.
29. Ghimire H, Venkataramani M, Bian Z, Liu Y, Perera AGU. ATR-FTIR spectral discrimination between normal and tumorous mouse models of lymphoma and melanoma from serum samples. Sci Rep [Internet]. 2017;7(1):1–9. Available from: http://dx.doi.org/10.1038/s41598-017-17027-4
30. Stapelfeldt K, Stamboroski S, Walter I, Suter N, Kowalik T, Michaelis M et al. Controlling the multiscale structure of nanofibrous fibrinogen scaffolds for wound healing. Nano Lett. 2019;19(9): 6554–63.
31. Das RK, Gocheva V, Hammink R, Zouani OF, Rowan AE. Stress-stiffening-mediated stem-cell commitment switch in soft responsive hydrogels. Nat Mater. 2016;15(3):318–25.

We are grateful to the all related institutions, especially Directorate General of Higher Education, Research, and Technology of the Republic of Indonesia for funding supports within State Contract No 090/E5/PG.02.00.PL/2024.

Gustini Gustini: https://orcid.org/0009-0002-8636-6857

Kaprawi Sahim: https://orcid.org/0000-0002-5297-5761

Ida Sriyanti: https://orcid.org/0000-0001-8011-8866

Irmawan Irmawan: https://orcid.org/0000-0002-6003-2333